Inorg. Chem. **XXXX**, *xx*, 0

Novel Luminescent Metal-Organic Frameworks $[Eu_2L_3(DMSO)_2(MeOH)_2]\cdot 2DMSO\cdot 3H_2O$ and $[Zn_2L_2(DMSO)_2]\cdot 1.6H_2O$ (L = 4,4′-Ethyne-1,2-diyldibenzoate)

Bich Tram Nguyen Pham, Liisa M. Lund, and Datong Song*

Davenport Chemical Research Laboratories, Department of Chemistry, University of Toronto, 80 St. George Street, Toronto, Ontario, Canada M5S 3H6

Received March 1, 2008

Novel metal-organic frameworks $[Eu_2L_3(DMSO)_2(MeOH)_2]\cdot 2DMSO\cdot 3H_2O$, **1**, and $[Zn_2L_2(DMSO)_2]\cdot 1.6H_2O$, **2**, (L = 4,4′-ethyne-1,2-diyldibenzoate) have been synthesized and structurally characterized. Compound **1** is a 3D open framework while **2** features interpenetrating 2D sheets in the crystal lattice. Both compounds have been characterized with X-ray crystallography, elemental analysis, and thermogravimetric analysis. Compounds **1** and **2** are red and blue-green luminescent, respectively, in the solid state at ambient temperature. Thermogravimetric analysis implies that the extensive interpenetration stabilizes the lattice of **2**, although it diminishes the porosity at the same time. The luminescence of **1** can be reversibly quenched and restored by the addition and removal of iodine.

Introduction

Metal-organic frameworks (MOFs) are an important class of materials[1] with applications in many areas, such as gas storage,[2] separation,[3] catalysis,[4] and sensing.[5] Because of the existence of well defined channels and large surface area, 3D open MOFs resemble zeolites both structurally and functionally. Owing to the nature of the construction, MOFs have many advantages over pure inorganic zeolites. For example, the use of organic ligands as the skeleton allows not only the fine-tuning of the size and shape of the void but also the interior decoration with various functional groups.[3e] Such fine-tuning ability renders MOFs more useful than pure inorganic zeolites for molecular recognitions.

Recently, luminescent MOFs with well defined open channels have been used as chemo-sensors with luminescence signal modulation as the reporting mechanism.[5] Our group is interested in developing novel luminescent MOFs and exploring their potential applications as sensors and self-

* To whom correspondence should be addressed. E-mail: dsong@chem.utoronto.ca.

(1) (a) Maspoch, D.; Ruiz-Molina, D.; Veciana, J. *Chem. Soc. Rev.* **2007**, *36*, 770. (b) Cheetham, A. K.; Rao, C. N. R.; Feller, R. K. *Chem. Commun.* **2006**, 4780. (c) Mueller, U.; Schubert, M.; Teich, F.; Puetter, H.; Schierle-Arndt, K.; Pastre, J. *J. Mater. Chem.* **2006**, *16*, 626. (d) Rowsell, J. L. C.; Yaghi, O. M. *Angew. Chem., Int. Ed.* **2005**, *44*, 4670. (e) Custelcean, R.; Moyer, B. A. *Eur. J. Inorg. Chem.* **2007**, 1321. (f) Lin, W. *J. Solid State Chem.* **2005**, *178*, 2486. (g) Ockwig, N. W.; Delgado-Friedrichs, O.; O'Keeffe, M.; Yaghi, O. M. *Acc. Chem. Res.* **2005**, *38*, 176.

(2) Gas Storage (a): Ma, S.; Sun, D.; Simmons, J. M.; Collier, C. D.; Yuan, D.; Zhou, H.-C. *J. Am. Chem. Soc.* **2008**, *130*, 1012. (b) Collins, D. J.; Zhou, H.-C. *J. Mater. Chem.* **2007**, *17*, 3154. (c) Fang, Q.-R.; Zhu, G.-S.; Jin, Z.; Ji, Y.-Y.; Ye, J.-W.; Xue, M.; Yang, H.; Wang, Y.; Qiu, S.-L. *Angew. Chem., Int. Ed.* **2007**, *46*, 6638. (d) Sun, D.; Ma, S.; Ke, Y.; Collins, D. J.; Zhou, H.-C. *J. Am. Chem. Soc.* **2006**, *128*, 3896. (e) Wong-Foy, A. G.; Matzger, A. J.; Yaghi, O. M. *J. Am. Chem. Soc.* **2006**, *128*, 3494. (f) Férey, G.; Mellot-Draznieks, C.; Serre, C.; Millange, F.; Dutour, J.; Surblé, S.; Margiolaki, I. *Science* **2005**, *309*, 2040. (g) Chun, H.; Dybtsev, D. N.; Kim, H.; Kim, K. *Chem.—Eur. J.* **2005**, *11*, 3521.

(3) Separation (a): Pan, L.; Olson, D. H.; Ciemnolonski, L. R.; Heddy, R.; Li, J. *Angew. Chem., Int. Ed.* **2006**, *45*, 616. (b) Chen, B.; Liang, C.; Yang, J.; Contreras, D. S.; Clancy, Y. L.; Lobkovsky, E. B.; Yaghi, O. M.; Dai, S. *Angew. Chem., Int. Ed.* **2006**, *45*, 1390. (c) Custelcean, R.; Haverlock, T. J.; Moyer, B. A. *Inorg. Chem.* **2006**, *45*, 6446. (d) Pan, L.; Parker, B.; Huang, X.; Olson, D. H.; Lee, J.; Li, J. *J. Am. Chem. Soc.* **2006**, *128*, 4180. (e) Custelcean, R.; Gorbunova, M. G. *J. Am. Chem. Soc.* **2005**, *127*, 16362. (f) Matsuda, R.; Kitaura, R.; Kitagawa, S.; Kubota, Y.; Belosludov, R. V.; Kobayashi, T. C.; Sakamoto, H.; Chiba, T.; Takata, M.; Kawazoe, Y.; Mita, Y. *Nature* **2005**, *436*, 238. (g) Dinca, M.; Long, J. R. *J. Am. Chem. Soc.* **2005**, *127*, 9376. (h) Bourrelly, S.; Llewellyn, P. L.; Serre, C.; Millange, F.; Loiseau, T.; Férey, G. *J. Am. Chem. Soc.* **2005**, *127*, 13519. (i) Maji, T. K.; Uemura, K.; Chang, H.-C.; Matsuda, R.; Kitagawa, S. *Angew. Chem., Int. Ed.* **2004**, *43*, 3269. (j) Dybtsev, D. N.; Chun, H.; Yoon, S. H.; Kim, D.; Kim, K. *J. Am. Chem. Soc.* **2004**, *126*, 32. (k) Pan, L.; Adams, K. M.; Hernandez, H. E.; Wang, X.; Zheng, C.; Hattori, Y.; Kaneko, K. *J. Am. Chem. Soc.* **2003**, *125*, 3062.

(4) Catalysis (a): Pan, L.; Liu, H.; Lei, X.; Huang, X.; Olson, D. H.; Turro, N. J.; Li, J. *Angew. Chem., Int. Ed.* **2003**, *42*, 542. (b) Seo, J. S.; Whang, D.; Lee, H.; Jun, S. I.; Oh, J.; Jeon, Y. J.; Kim, K. *Nature* **2000**, *404*, 982. (c) Fujita, M.; Kwon, Y. J.; Washizu, S.; Ogura, K. *J. Am. Chem. Soc.* **1994**, *116*, 1151.

10.1021/ic800394g CCC: $40.75
Published on Web 06/25/2008

indicating gas storage materials. In a recent effort on constructing novel luminescent MOFs, we have used 4,4′-ethyne-1,2-diyldibenzoic acid (LH_2) to self-assemble with lanthanide(III) and Zn(II) salts, respectively. Luminescent compounds of these two types of metal ions have different features. Lanthanide(III) compounds usually luminesce via the ligand-promoted metal-centered excited states, which are populated by the photon energy harvested by the ligand through a ligand-to-metal energy transfer process. On the other hand, luminescent zinc(II) compounds usually exhibit ligand-centered emissions, in which the coordination to zinc(II) centers restricts the thermal motion of the ligand and thus, enhances the ligand-centered luminescence. Both types of luminescence signals can be modulated by certain environment changes, such as interactions between luminescent molecules and analyte molecules, giving both types of luminescent compounds sensing abilities. The reason for choosing LH_2 as the ligand is multifold. First, LH_2 is luminescent in both free and deprotonated forms; such luminescent properties can potentially be imparted to the corresponding MOFs. Second, the rigid, linear, ditopic ligand LH_2 has both aromatic ring and alkyne functionalities, which can potentially serve as the interacting sites for certain analyte molecules. Third, LH_2 is readily available through simple organic synthesis. Herein, we report the syntheses, structures, and luminescence properties of a Eu(III)-based 3D and a zinc(II)-based interpenetrating 2D MOFs derivatized from LH_2.

Experimental Section

General Information. Elemental analyses were performed at the Analyst of our Chemistry Department with a PE 2400 C/H/N/S analyzer. Thermogravimetric analyses (TGA) were performed on a TA Instruments SDT Q600 unit under a N_2 atmosphere with a heating rate of 2 °C per minute. Luminescence spectra were recorded on a Fluorolog-3 Jobin Yvon Horiba luminescence spectrometer equipped with a 450W xenon lamp. Unless otherwise stated, all manipulations were performed in air and all reagents were purchased from commercial sources and used without further purification. THF solvent for Sonogashira coupling was freshly distilled over Na/benzophenone; DBU and H_2O for the coupling reaction were degassed prior to use; the coupling reaction was carried out under an argon atmosphere using standard Schlenk techniques.

Synthesis of $[Eu_2L_3(DMSO)_2(MeOH)_2]\cdot 2DMSO\cdot 3H_2O$, 1. A solution of $EuCl_3\cdot 6H_2O$ (0.055 g, 0.150 mmol, in 4 mL of MeOH) was mixed with a solution of LH_2 (0.08 g, 0.3 mmol, in 12 mL of DMSO). The resulting mixture was filtered through Celite into a vial that is then inserted into a larger vial containing 200 mL of a 0.015 M Et_3N solution in MeOH/DMSO (1:1 by volume). The larger vial was sealed and left undisturbed for 17 days. The resulting colorless crystals of **1** were collected, washed with MeOH/DMSO (1:1 by volume), and air-dried (yield: 0.055 g, 48% based on $EuCl_3\cdot 6H_2O$). Anal. Calcd for $[Eu_2(DMSO)_2(MeOH)_2L_3]\cdot 2DMSO\cdot 2H_2O$ (due to partial solvent loss under vacuum): C, 46.16; H, 4.01. Found: C, 46.0; H, 3.70.

Synthesis $[Zn_2L_2(DMSO)_2]\cdot 1.6H_2O$, 2. A solution of $Zn(NO_3)_2\cdot 6H_2O$ (0.0168 g, 0.0563 mmol, in 3 mL of MeOH) was mixed with a solution of LH_2 (0.0151 g, 0.0564 mmol, in 2 mL of DMSO). The resulting mixture was filtered through Celite into a vial that was then inserted into a larger vial containing 30 mL of a 0.015 M solution of Et_3N in MeOH/DMSO (1:1 by volume). The larger vial was sealed and left undisturbed for 14 days. Off-white crystals of **2** were collected, washed with MeOH/DMSO (1:1 by volume), and air-dried (yield: 4.4 mg, 18% based on $Zn(NO_3)_2\cdot 6H_2O$). Anal. Calcd for $Zn_2C_{36}H_{31.2}O_{11.6}S_2$: C, 51.23; H, 3.70. Found: C, 51.37; H, 3.46.

X-ray Crystallographic Analysis. X-ray quality single crystals of **1** and **2** were obtained as described in the sections above. All crystals were mounted on the tip of a MiTeGen MicroMount. All single-crystal X-ray diffraction data were collected on a Nonius Kappa-CCD diffractometer with Mo Kα radiation ($\lambda = 0.71073$ Å), operating at 50 kV and 30 mA, at 150 K controlled by an Oxford Cryostream 700 series low temperature system. The data integration and absorption correction were performed with the DENZO-SMN package.[6] All structures were solved by the direct methods and refined using SHELXTL V6.10.[7] Crystals of **1** belong to the monoclinic space group $P2_1/c$ while crystals of **2** belong to the orthorhombic space group *Pbca*. The coordinated DMSO molecules in both structures are disordered over two orientations; such disordering has been modeled successfully. Crystals of **1** contain partially escaped DMSO and water molecules in the open channels while crystals of **2** contain partially escaped water molecules in the cavities. If the SQUEEZE function of the PLATON software package[8] is used to remove the electron density from the channels of **1**, the R_1 and wR_2 factors can be improved significantly. Therefore, the high wR_2 factor for **1** is likely caused by the diffused electron density from the disordered solvent molecules in the cavities. For the same reason, ChECK-CIF reports a level-B alert on a solvent accessible void of 3%. All non-hydrogen atoms from the main molecules and some of the cavity solvent molecules were refined with anisotropic thermal parameters. The positions of hydrogen atoms (except those involved in the disordered portions and those attached to oxygen atoms) were calculated with the riding model and their contributions were included in the structure factor calculations. The crystallographic data of **1** and **2** are summarized in Table 1 while the selected bond lengths and angles are shown in Tables 2 and 3, respectively.

Results and Discussion

Syntheses and Structures. The free ligand LH_2 can be synthesized in good yield (Scheme 1) through a modified Sonogashira coupling reaction of methyl 4-iodobenzoate and trimethylsilyl acetylene,[9a] followed by hydrolysis under basic conditions.[9b] Our experiments indicate that the quality of DBU affects the yield of the coupling reaction significantly.

(5) Sensing (a): Chen, B.; Yang, Y.; Zapata, F.; Lin, G.; Qian, G.; Lobkovsky, E. B. *Adv. Mater.* **2007**, *19*, 1693. (b) Bauer, C. A.; Timofeeva, T. V.; Settersten, T. B.; Patterson, B. D.; Liu, V. H.; Simmons, B. A.; Allendorf, M. D. *J. Am. Chem. Soc.* **2007**, *129*, 7136. (c) Zhao, B.; Gao, H.-L.; Chen, X.-Y.; Cheng, P.; Shi, W.; Liao, D.-Z.; Yan, S.-P.; Jiang, Z.-H. *Chem. Eur. J.* **2006**, *12*, 149. (d) Liu, W.; Jiao, T.; Li, Y.; Liu, Q.; Tan, M.; Wang, H.; Wang, L. *J. Am. Chem. Soc.* **2004**, *126*, 2280. (e) Zhao, B.; Chen, X.-Y.; Cheng, P.; Liao, D.-Z.; Yan, S.-P.; Jiang, Z.-H. *J. Am. Chem. Soc.* **2004**, *126*, 15394. (f) Lefebvre, J.; Batchelor, R. J.; Leznoff, D. B. *J. Am. Chem. Soc.* **2004**, *126*, 16117.

(6) Otwinowski, Z.; Minor, W. *Methods Enzymol.* **1997**, *276*, 307.

(7) Sheldrick, G. M. *SHELXTL/PC, Version 6.1 Windows NT Version*; Bruker AXS Inc.: Madison, WI, 2001.

(8) (a) Spek, A. L. *Acta Crystallogr.* **1990**, *A46*, C34. (b) Spek, A. L. PLATON, *A Multipurpose Crystallographic Tool*; Utrecht University: Utrecht, The Netherlands, 2000.

Table 1. Crystallographic Data of **1** and **2**

	1	**2**
formula	$C_{54}H_{44}O_{16}S_2Eu_2 \cdot 2DMSO \cdot 3H_2O$	$C_{36}H_{28}O_{10}S_2Zn_2 \cdot 1.6H_2O$
FW	1527.26	844.27
T (K)	150(2)	150(2)
space group	$P2_1/c$	$Pbca$
a (Å)	10.4299(2)	15.8816(4)
b (Å)	13.5219(3)	9.2974(2)
c (Å)	31.6642(6)	25.2870(7)
α (°)	90	90
β (°)	97.6208(13)	90
γ (°)	90	90
V (Å^3)	4426.22(15)	3733.82(16)
Z	2	4
ρ_{calcd} (g·cm^{-3})	1.144	1.502
μ (mm^{-1})	1.551	1.456
F(000)	1532	1728
reflns collected	30183	25097
independent. reflns	7787	3271
no. of parameters	420	247
R [$I > 2\sigma(I)$]	$R_1 = 0.0776$	$R_1 = 0.0551$
	$wR_2 = 0.2299$	$wR_2 = 0.1458$
R (all data)	$R_1 = 0.1045$	$R_1 = 0.0756$
	$wR_2 = 0.2589$	$wR_2 = 0.1612$
GOF on F^2	1.044	1.084

Table 2. Selected Bond Lengths (Å) and Angles (deg) of **1**

Eu(1)−O(5A)	2.351(7)	O(6)−Eu(1)−O(4)	132.6(2)
Eu(1)−O(1)	2.385(6)	O(5A)−Eu(1)−O(7)	77.9(3)
Eu(1)−O(2A)	2.403(6)	O(1)−Eu(1)−O(7)	134.1(3)
Eu(1)−O(8)	2.405(7)	O(2A)−Eu(1)−O(7)	74.5(3)
Eu(1)−O(6)	2.416(6)	O(8)−Eu(1)−O(7)	75.1(3)
Eu(1)−O(4)	2.426(6)	O(6)−Eu(1)−O(7)	143.9(3)
Eu(1)−O(7)	2.463(8)	O(4)−Eu(1)−O(7)	69.7(3)
Eu(1)−O(3)	2.586(6)	O(5A)−Eu(1)−O(3)	131.3(2)
Eu(1)−O(5)	2.806(6)	O(1)−Eu(1)−O(3)	69.7(2)
O(5A)−Eu(1)−O(1)	73.1(2)	O(2A)−Eu(1)−O(3)	150.7(2)
O(5A)−Eu(1)−O(2A)	78.0(2)	O(8)−Eu(1)−O(3)	73.7(2)
O(1)−Eu(1)−O(2A)	130.6(2)	O(6)−Eu(1)−O(3)	81.6(2)
O(5A)−Eu(1)−O(8)	148.2(2)	O(4)−Eu(1)−O(3)	51.7(2)
O(1)−Eu(1)−O(8)	138.6(2)	O(7)−Eu(1)−O(3)	107.3(3)
O(2A)−Eu(1)−O(8)	78.8(2)	O(5A)−Eu(1)−O(5)	73.7(2)
O(5A)−Eu(1)−O(6)	123.0(2)	O(1)−Eu(1)−O(5)	67.0(2)
O(1)−Eu(1)−O(6)	82.0(2)	O(2A)−Eu(1)−O(5)	66.9(2)
O(2A)−Eu(1)−O(6)	81.3(2)	O(8)−Eu(1)−O(5)	116.0(2)
O(8)−Eu(1)−O(6)	74.1(3)	O(6)−Eu(1)−O(5)	49.4(2)
O(5A)−Eu(1)−O(4)	89.1(2)	O(4)−Eu(1)−O(5)	141.4(2)
O(1)−Eu(1)−O(4)	75.0(2)	O(7)−Eu(1)−O(5)	135.7(3)
O(2A)−Eu(1)−O(4)	143.8(2)	O(3)−Eu(1)−O(5)	117.0(2)
O(8)−Eu(1)−O(4)	96.9(3)		

Table 3. Selected Bond Lengths (Å) and Angles (deg) for **2**

Zn(1)−O(5)	1.981(4)	O(5)−Zn(1)−O(2A)	99.23(16)
Zn(1)−O(3)	2.009(3)	O(3)−Zn(1)−O(2A)	90.60(15)
Zn(1)−O(4A)	2.043(4)	O(4A)−Zn(1)−O(2A)	87.97(15)
Zn(1)−O(2A)	2.060(3)	O(5)−Zn(1)−O(1)	101.01(15)
Zn(1)−O(1)	2.072(4)	O(3)−Zn(1)−O(1)	89.85(16)
O(5)−Zn(1)−O(3)	103.62(15)	O(4A)−Zn(1)−O(1)	83.96(16)
O(5)−Zn(1)−O(4A)	97.95(15)	O(2A)−Zn(1)−O(1)	159.05(16)
O(3)−Zn(1)−O(4A)	158.33(16)		

Compound **1** can be prepared in crystalline form in 40−50% yield by diffusing triethylamine vapor into the mixed solution of LH_2 and the corresponding $EuCl_3 \cdot 6H_2O$

Scheme 1. Synthesis of LH_2

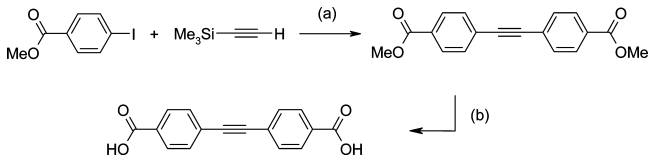

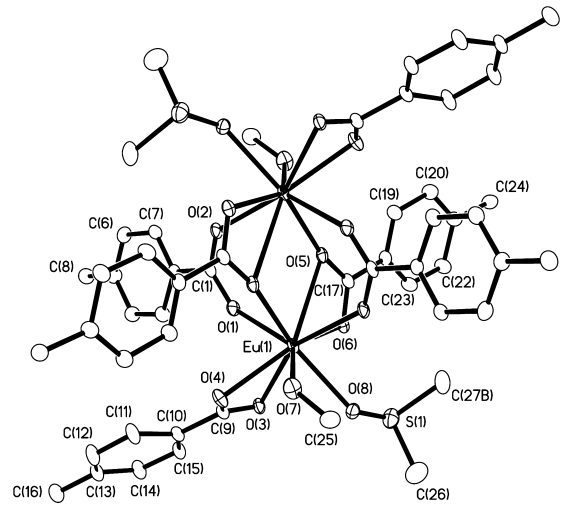

Figure 1. X-ray structure of a $[Eu_2L_3(MeOH)_2(DMSO)_2]$ unit in compound **1**, with thermal ellipsoids plotted at 15% probability. Hydrogen atoms are omitted, and the disordered DMSO ligands are plotted in one orientation for clarity.

Scheme 2. Coordination Modes of the L^{2-} Ligand

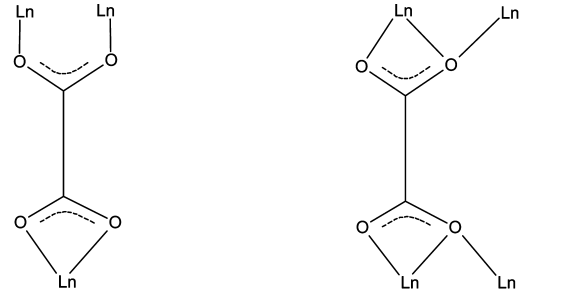

mode 1: bridging (top) and chelating (bottom) mode 2: chelate-bridging (both ends)

at ambient temperature. It is insoluble in common solvents. An unidentified white amorphous solid is also obtained as a byproduct consistently.

Compound **1** is a 3D coordination polymer in the solid state with dinuclear metal-containing units, formulated as $[Eu_2L_3(MeOH)_2(DMSO)_2]$, cross-linked together by sharing linear linker ligands, L^{2-}. The framework is charge neutral. As shown in Figure 1, there is a crystallographically imposed center of inversion in the middle of the $[Eu_2L_3(MeOH)_2(DMSO)_2]$ unit. Within each $[Eu_2L_3(MeOH)_2(DMSO)_2]$ unit, the carboxylate groups of the L^{2-} ligands display three different coordination modes: the chelating mode (O(3)−C(9)−O(4)), the bridging mode (O(1)−C(1)−O(2)), and the "chelate-bridging" mode (O(5)−C(17)−O(6)). The L^{2-} ligands display two coordination modes in the crystal lattice (Scheme 2): (1) one of the two carboxylate groups adopts the chelating mode while the other carboxylate group adopts the bridging mode; (2) both carboxylate groups adopt the "chelate-bridging" mode.

Each Eu(III) center is 9-coordinate, showing a distorted tricapped trigonal prismatic coordination geometry (Figure 2). In addition to the 7 oxygen donor atoms from the L^{2-} ligands, a methanol and DMSO terminal ligands contribute 2 oxygen donor atoms to the coordination sphere. The two triangular faces of the distorted trigonal prism are defined by [O(2A), O(6), O(8)] and [O(1), O(4), O(5A)], respec-

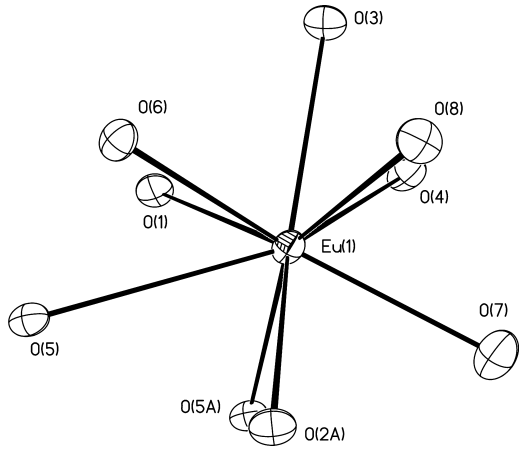

Figure 2. Structure of the coordination sphere of Eu(1) center, showing the tricapped trigonal prismatic coordination geometry.

tively, while the three rectangular faces are capped by O(3), O(5), and O(7), respectively. The two triangular faces of the distorted trigonal prism are unparallel with a dihedral angle of ~12°. The sum of the bond angles, O(3)−Eu(1)−O(5), O(3)−Eu(1)−O(7), and O(5)−Eu(1)−O(7) is 360.0(3)°. The longest Eu−O bond in compound **1** is Eu(1)−O(5), with a bond length of 2.806(6) Å, as a result of the unsymmetrical sharing of O(5) between the two Eu(III) centers, similar to the literature values.[10] The remaining Eu−O bonds are in the range of 2.351(7)−2.586(6) Å, comparable to the reported bond lengths.[10] The distance between the two Eu(III) centers is 4.1367(9) Å, in the reported range for similar structural units.[10e]

As shown in Figure 3a, each $[Eu_2L_3(MeOH)_2(DMSO)_2]$ unit shares its L^{2-} ligands with six neighboring units, leading to the formation of a 3D framework in the extended structure of **1**. There are 1D triangular open channels along the *a* axis in the crystal lattice of **1**, filled with DMSO and water solvent molecules. The spacefilling model of a 1D channel is shown in Figure 3b. The longest base and the corresponding height of the triangular opening are approximately 7.5 and 4.5 Å, respectively. The 1D channels are defined by the aromatic rings and the CC triple bonds of the L^{2-} ligands. The solvent accessible void formed by the MOF skeleton calculated by the Platon software package[8] is 49%.

Crystals of compound **2** can be prepared by diffusing triethylamine vapor into a mixture of LH_2 and $Zn(NO_3)_2 \cdot 6H_2O$ in DMSO/methanol. Similar to **1**, compound **2** is insoluble in common solvents. An unidentified needle-like byproduct is produced from the same reaction, which is also insoluble in common solvents.

Compound **2** forms interpenetrating 2D sheets in the solid state. Each 2D sheet consists of ligand-sharing $[Zn_2L_2(DMSO)_2]$ units, the structure of which is shown in Figure 4a. Each $[Zn_2L_2(DMSO)_2]$ unit consists of two Zn(II) centers bridged by four carboxylate groups from L^{2-} ligands in a paddle-wheel fashion. There is a crystallographically imposed center of inversion in the middle of each paddle-wheel unit. Similar paddle-wheel building blocks have been reported in the literature.[11] Each Zn(II) center adopts a pseudo square-pyramidal coordination geometry, with four carboxylate oxygen donor atoms, O(1), O(2A), O(3), and O(4A), occupying four corners of the square-base and an oxygen donor atom, O(5), from the terminal DMSO ligand occupying the apex of the pyramid. The length of Zn(1)−O(5) bond is 1.984(3) Å, slightly shorter than the Zn−O bonds in the square-base (avg. 2.046(3) Å). The Zn(II) center is ~0.37 Å out of plane of the square-base toward the apex of the pyramid. The average angle between the Zn(1)−O(5) bond and the Zn−O bonds in the square-base is 100.5(2)°, comparable to the literature values.[11] The distance between the two Zn(II) centers within a $[Zn_2L_2(DMSO)_2]$ unit is 2.9786(9) Å, similar to the distances reported for the paddle-wheel units in the literature.[11]

As shown in Figure 4b, each $[Zn_2L_2(DMSO)_2]$ paddle-wheel unit shares its L^{2-} ligands with four adjacent units to form an extended 2D sheet in the crystal lattice of **2**. The terminally coordinated DMSO molecules appear to prevent further cross-linking and therefore, the third dimension is not observed. Unlike in compound **1**, where the L^{2-} ligands are linear, the L^{2-} ligands are slightly curved in compound **2**. Therefore, the structure of a 2D sheet can also be viewed as a set of edge-sharing "tiles" with complementary shapes.

Figure 5a shows a set of parallel 2D sheets stacking along the *b* axis in the crystal lattice. The spacing between two adjacent sheet-planes is ~6 Å, where a sheet-plane is defined by the centroids of all the paddle-wheel units within one 2D sheet. Two sets of such 2D sheets coexist in the lattice of **2**; they both stack along the *b* axis with different orientations as illustrated in Figure 5b. The dihedral angle between the two sets of sheet-planes is ~81°. As shown in Figure 6, the two sets of 2D sheets interpenetrate each other in the crystal lattice, blocking the 1D channels formed by each individual stack of sheets, leaving only small interstitial cavities where water molecules reside. The solvent accessible void between the skeleton of **2** caculated with the Platon[8] software package is 14%. There are π-π stacking interactions between the aromatic rings of the interpenetrating 2D sheets, with the short contact distance of ~3.5 Å.

Although LH_2 has been reported for over two decades,[12] to the best of our knowledge, it has never been incorporated into a metal-organic-framework to date. This ligand is longer

(9) (a) Mio, M. J.; Kopel, L. C.; Braun, J. B.; Gadzikwa, T. L.; Hull, K. L.; Brisbois, R. G.; Markworth, C. J.; Grieco, P. A. *Org. Lett.* **2002**, *4*, 3199. (b) Fasina, T. M.; Collings, J. C.; Burke, J. M.; Batsanov, A. S.; Ward, R. M.; Albesa-Jové, D.; Porrès, L.; Beeby, A.; Howard, J. A. K.; Scott, A. J.; Clegg, W.; Watt, S. W.; Viney, C.; Marder, T. B. *J. Mater. Chem.* **2005**, *15*, 690.

(10) (a) Cahill, C. L.; de Lill, D. T.; Frisch, M. *CrystEngComm* **2007**, *9*, 15. (b) Yang, X.-P.; Jones, R. A.; Rivers, J. H.; Lai, R. P.-j. *Dalton Trans.* **2007**, 3936. (c) Hong, X.-L.; Li, Y.-Z.; Hu, H.; Pan, Y.; Bai, J.; You, X.-Z. *Cryst. Growth Des.* **2006**, *6*, 1221. (d) de Bettencourt-Dias, A.; Viswanathan, S. *Dalton Trans.* **2006**, 4093. (e) Viswanathan, S.; de Bettencourt-Dias, A. *Inorg. Chem.* **2006**, *45*, 10138.

(11) (a) Fang, Q.; Zhu, G.; Xue, M.; Sun, J.; Sun, F.; Qiu, S. *Inorg. Chem.* **2006**, *45*, 3582. (b) Chun, H.; Dybtsev, D. N.; Kim, H.; Kim, K. *Chem.—Eur. J.* **2005**, *11*, 3521. (c) Dybtsev, D. N.; Chun, H.; Kim, K. *Angew. Chem., Int. Ed.* **2004**, *43*, 5033; *Angew. Chem.* **2004**, *116*, 5143. (d) Eddaoudi, M.; Kim, J.; Vodak, D.; Sudik, A.; Wachter, J.; O'Keeffe, M.; Yaghi, O. M. *Proc. Natl. Acad. Sci. U. S. A.* **2002**, *99*, 4900. (e) Kim, J.; Chen, B.; Reineke, T. M.; Li, H.; Eddaoudi, M.; Moler, D. B.; O'Keeffe, M.; Yaghi, O. M. *J. Am. Chem. Soc.* **2001**, *123*, 8239.

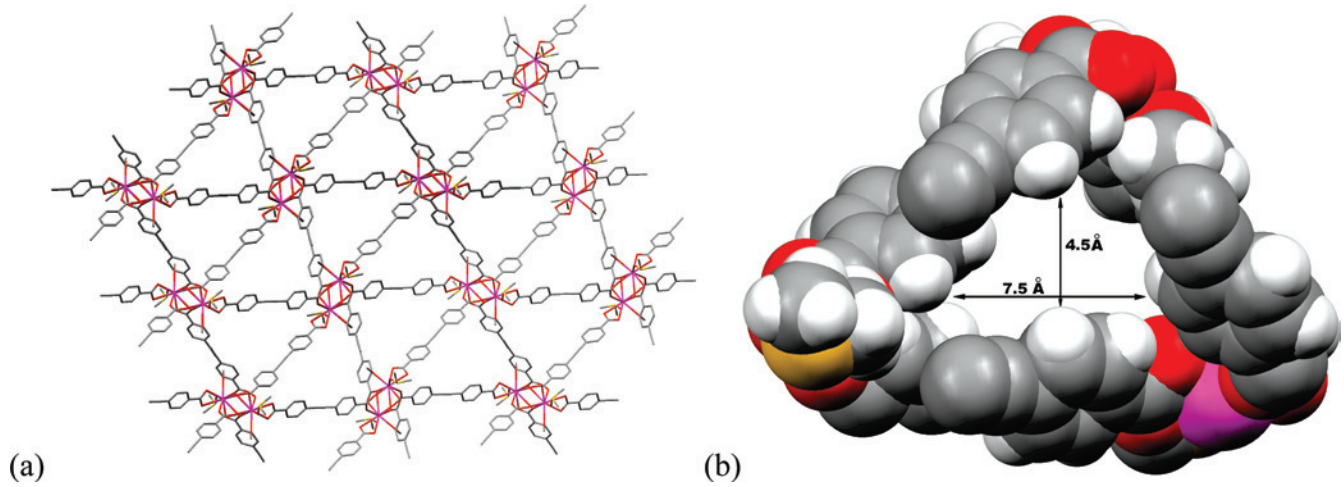

Figure 3. (a) Projection down the *a* axis, showing the 1D triangular open channels in the lattice of **1**. All hydrogen atoms and solvent molecules in the channel are omitted for clarity. (b) Spacefilling model of one channel, showing the dimension.

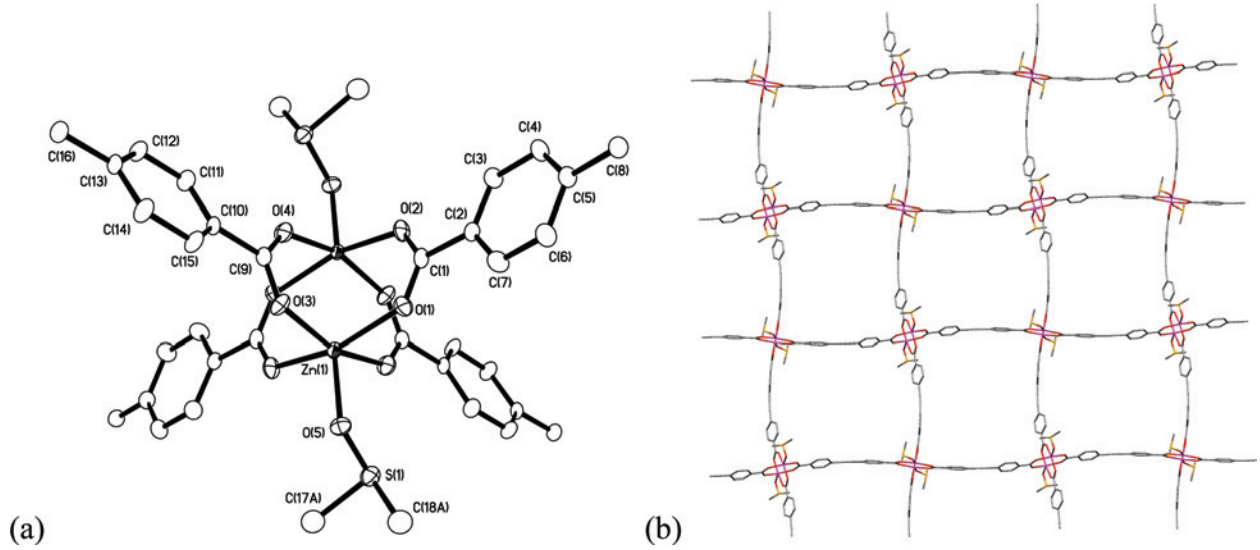

Figure 4. (a) Structure of a $[Zn_2L_2(DMSO)_2]$ paddle-wheel unit in **2**, with the thermal ellipsoids plotted at 30% probability. (b) The top view of a 2D sheet. The disordered DMSO molecules are shown in one set of coordinates and all hydrogen atoms are omitted for clarity.

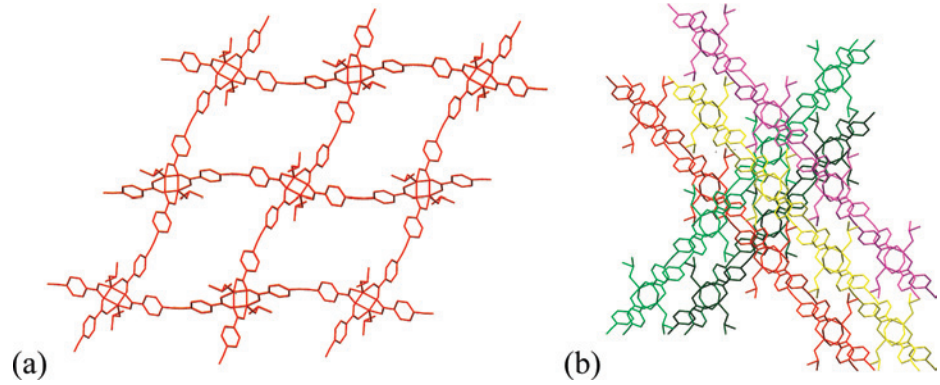

Figure 5. (a) Projection diagram down the *b* axis, showing the stacking of one set of 2D sheets in the lattice of **2**. (b) A projection diagram down the *c* axis, showing the two sets of 2D sheets with two orientations. The disordered DMSO molecules are shown in one set of coordinates and water molecules and hydrogen atoms are omitted for clarity.

than the 1,4-benzenedicarboxylate (BDC) ligand because of the extra CC triple bond between the two phenyl groups. This increase in length does not cause the formation of interpenetrating 3D frameworks in the cases of **1**. In contrast, Yaghi and co-workers have reported that the use of a long dicarboxylate linker, 4,4′-azodibenzoate (ADB), produces an interpenetrating 3D framework, formulated as $Tb_2(ADB)_3(DMSO)_4 \cdot 16DMSO$.[13] In the case of compound **2**, however, extensive interpenetration has been observed, which diminishes the void space significantly.

Thermogravimetric Analysis (TGA). The TGA curves for compounds **1** and **2** are shown in the Supporting

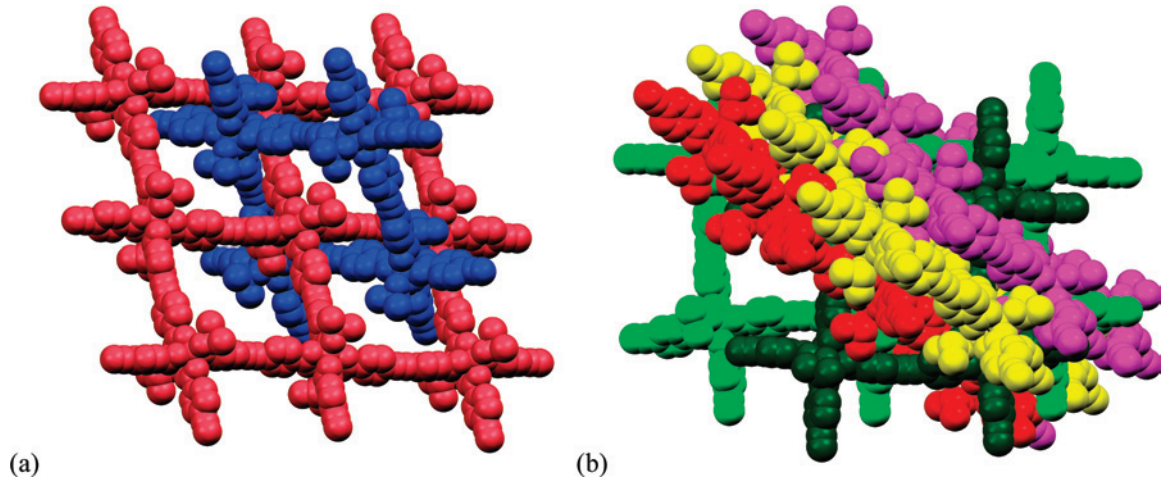

Figure 6. Spacefilling diagrams showing the interpenetrating 2D sheets in the lattice of **2**. Each sheet is plotted in a distinct color. (a) One sheet per direction, demonstrating the interpenetration; (b) three sheets in one direction (red, yellow, and purple) and two sheets in the other direction (light and dark green), showing the complete blockage of the channels.

Information, Figure 1S. Compound **1** loses solvent molecules from the channels and the metal centers between 20 and 120 °C, showing a 28% weight loss, consistent with the calculated results. At a higher temperature, the L^{2-} ligands start to escape. Compound **2** loses all the lattice water molecules between 20 and 120 °C, showing a 3.4% weight loss, consistent with the calculated value. It loses half of its terminal DMSO ligands (1 DMSO molecule per paddle-wheel unit, ca. 9.2% weight) from 120 to 210 °C, showing a 9.2% weight loss. Between 210 and 415 °C, the remaining DMSO ligands (1 DMSO molecule per paddle-wheel unit, ca. 9.2% weight) escape slowly, showing a further weight loss of 9.2%. Above 415 °C, the L^{2-} ligands start to escape or decompose.

The TGA results indicate that **2** is more robust than **1** with respect to solvent loss, consistent with the prediction on the basis of the crystal structures. The cocrystallized water molecules and the terminal DMSO ligands in **2** are tightly trapped by the interpenetrating 2D sheets and thus require higher temperature to escape the crystal lattice. The interpenetration also appears to make the skeleton of the framework more stable with respect to the loss of the L^{2-} ligands, presumably because of the multiple π-π stacking interactions between the aromatic rings in the lattice of **2**.

Luminescence Properties. The photoluminescence excitation and emission spectra of Na_2L (in a 150 μM aqueous solution and in the solid state), **1**, and **2** (in the solid states) at 25 °C are shown in Figure 7. The L^{2-} ligand (in the form of its sodium salt, in aqueous solution) is a weak purple-blue emitter, showing a broadband emission between 330 and 500 nm with the emission maximum at 355 nm (excited at 328 nm, the excitation maximum). In the solid state, Na_2L has a broadband emission that covers almost the entire visible region with the emission maximum at 437 nm (excited at 375 nm).[14] The red shift compared to the solution spectrum is presumably due to the intermolecular interactions (such as π-π stacking) between the molecules in the solid state. Crystals of **1** display intense red luminescence under UV irradiation at ambient temperature. The sharp emission spectrum (excited at 360 nm)[14] is characteristic for the Eu(III)-based luminescence with three maxima at 593, 615, and 698 nm, which are from the $^5D_0 \rightarrow {}^7F_1$, $^5D_0 \rightarrow {}^7F_2$, and $^5D_0 \rightarrow {}^7F_4$ transitions, respectively.[15] No ligand-based emission is observed, indicating an efficient ligand-to-metal energy transfer process. Crystals of **2** have bright luminescence that appears blue-green to the naked eye. The broadband emission of **2** (excited at 375 nm)[14] covers almost the entire visible region with two maxima at 411 and 487 nm. Similar to that observed for Na_2L solid, the red shift displayed by **2** in the solid state relative to L^{2-} in solution is presumably caused by the intermolecular interactions, such as π-π stacking interactions, in the crystal lattice.

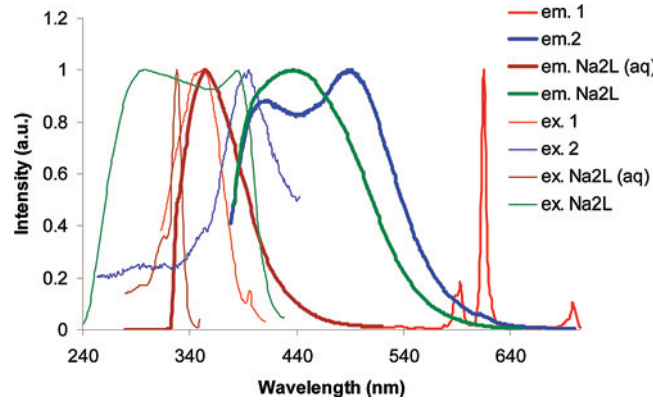

Figure 7. Photoluminescence excitation (thin lines) and emission (thick lines) spectra of **1**, **2**, and Na_2L at 25 °C with normalized intensities. For each sample, the excitation and emission curves have the same color. Except for the spectra of Na_2L (aq), which were recorded for a 150 μM aqueous solution sample, all other spectra were recorded for solid samples.

To test the response in luminescence signal from **1** upon binding of small molecules, iodine has been chosen because it is known to form a charge transfer complex with aromatic rings.[16] If iodine binds to the ligand moieties in **1**, the ligand-to-metal energy transfer process will be disrupted, and the metal centered emission quenched. Indeed, when the white crystals of **1** are soaked in a purple solution of iodine in

(12) Lee, B. H.; Marvel, C. S. *J. Polym. Sci., Part A: Polym. Chem. Ed.* **1982**, *20*, 393.
(13) Reineke, T. M.; Eddaoudi, M.; Moler, D.; O'Keeffe, M.; Yaghi, O. M. *J. Am. Chem. Soc.* **2000**, *122*, 4843.

hexanes, the white crystals become yellow-orange (the characteristic color for a charge transfer complex formed by iodine)[16] rapidly, with the complete loss of luminescence. The single crystal X-ray diffraction analysis on the resulting yellow-orange crystals reveals a structure with identical skeleton as in **1**. The low level of iodine binding is likely random, and therefore, the disordering does not allow the observation of iodine in the crystal structure. The yellow-orange crystals can be soaked and washed with DMSO a few times to regenerate the white crystals of **1**, and the red luminescence is also restored with the washing process. The luminescence quenching and restoring cycle can be repeated, although the quality of the crystals becomes worse and eventually the crystals cannot be used for X-ray diffraction analysis. Although the iodine binding sites and modes are yet to be investigated (e.g., surface vs channel binding; triple bond vs aromatic ring), the reversible luminescence signal modulations by the addition and removal of iodine suggest the possibility of using **1** as a luminescent sensor.

Summary

We have synthesized two novel metal-organic frameworks using a luminescent linear dicarboxylate ligand, L^{2-}. The Eu(III) compound, **1**, is a 3D open framework while the Zn(II) compound, **2**, features the interpenetrating 2D sheets structure. Both compounds are insoluble in common solvents, consistent with the extended network structures. Both **1** and **2** are luminescent at ambient temperature in the solid states. The solvent channels found in **1** are defined by the extended π-system of the ligand, with exposed CC triple bonds and aromatic rings. Such structure motifs can potentially serve as the guest binding sites for molecular recognition. The binding of guest molecules can potentially alter the energy transfer process from the ligands to the metal centers and, in turn, cause luminescence signal modulation. Such luminescence signal modulations have been demonstrated by the preliminary iodine binding experiments. Although iodine-sensing is not of much practical significance, the experiments do suggest the possibility of using **1** as a luminescent sensor, where the linker group of the ligand is possibly the binding site. The terminal DMSO ligands in compound **2** appear to prevent the formation of a 3D framework. Replacing DMSO with a ditopic linear linker ligand may further cross-link the 2D sheets into a 3D framework. The nature of the iodine binding with **1**, the possibilities of constructing 3D MOFs as luminescent sensors using the L^{2-} ligand, and using appropriate linker ligands to replace the DMSO ligands in **2** to build novel luminescent 3D frameworks are being explored in our laboratory.

Acknowledgment. This research is supported by grants to D.S. from the Natural Science and Engineering Research Council (NSERC) of Canada, Canadian Foundation for Innovation (CFI), Ontario Ministry of Research Innovation, Connaught Foundation, and the University of Toronto. The Nitz, Winnik, and Ozin groups are thanked for sharing instrumentations. Dr. Georgeta Masson is thanked for assistance on TGA measurements.

Supporting Information Available: Crystallographic data for **1** and **2** in cif format and the TGA curves (PDF). This material is available free of charge via the Internet at http://pubs.acs.org.

IC800394G

(14) The excitation wavelength was chosen with two criteria: (a) close to the excitation maximum to achieve high emission intensity; (b) avoid the interference of the incident light scattering peaks, including the higher order ones.

(15) Lakowicz, J. R. *Principles of Fluorescence Spectroscopy*, 2nd ed.; Kluwer Academic/Plenum Publishers: New York, 1999.

(16) Housecroft, C. E., Sharpe, A. G. *Inorg. Chem.* 2nd ed.; Pearson Education Limited: England, 2005.